Discharge coefficient of a broad crested side weir in an earthen channel

Mohammad Reza Namaee, Mohammad Sadegh Jalaledini, Mahdi Habibi, Saeed Reza Sabbagh Yazdi and Mona Ghafouri Azar

ABSTRACT

Side weirs are widely used to divert flows from rivers and channels. However, the hydraulic behavior of this type of weir is complex and difficult to predict accurately. Previous studies on side weirs have generally focused on side weirs in rectangular channels with a smooth bed. However, one of the applications of side weirs is in irrigation systems which have trapezoidal cross sections and significant bed roughness. The present study investigates the hydraulic behavior of a broad crested side weir in an earthen channel with a rough bed under subcritical flow. These investigations showed that the side weir discharge coefficient is influenced by four main parameters which are upstream Froude number, ratio of the main channel width to the upstream flow depth, ratio of the length of the side weir to the main channel width and ratio of side weir height to the upstream flow depth. The results showed that the discharge coefficient of the side weir gives a lower coefficient value compared to other researchers' equations. Nearly 90 experimental tests were carried out and finally new equations are proposed for prediction of discharge coefficient of a broad crested side weir in an earthen channel under subcritical conditions which can be mainly used in common irrigation systems.

Key words | discharge coefficient, earthen channel, side weir, subcritical

Mohammad Reza Namaee (corresponding author)
Khaje Nasir Toosi University of Technology,
Tehran,
Iran
E-mail: *mnemaie@yahoo.com*

Mohammad Sadegh Jalaledini
Mahdi Habibi
Soil Conservation and Watershed Management
    Research Institute,
Tehran,
Iran

Saeed Reza Sabbagh Yazdi
Civil Engineering Department,
KN Toosi University of Technology,
Tehran,
Iran

Mona Ghafouri Azar
University of Tehran,
Karaj,
Iran
Postal address: Tehran,
Karaj Special Road Km 10,
St. Ashry martyr - martyr Shafiee St.,
PO Box 1136-13445

NOTATION

A	Cross-sectional area of flow	y	Water depth in main channel
T	Top width of flow	y_C	Critical water depth in main channel
B	Main width of the channel	α	Kinetic energy coefficient
C_M	De Marchi coefficient of discharge	g	Gravitational acceleration
L	Weir length	dy/dx	Slope of the water surface profile
E	Specific energy	σ	Surface tension
Q_S	Weir outflow discharge		
$Q_{in,1}$	Upstream discharge		
Q_2	Downstream discharge		
Q	Discharge per unit length over weir		
Fr	Froude number		
S_f	Energy line slope		
S_0	Channel slope		
P	Weir height		
x	Longitudinal direction		

INTRODUCTION

Side weirs are essentially weirs installed along the sides of the main channel to divert or spill excess water. Estimation of discharge over the side weirs is still an important issue and an ongoing problem in the area of water measurement. Prior to 1978, most of the studies were focused on the

empirical derivation of discharge formulas. Probably the first rational approach to studying side weir discharge was made by De Marchi (1934) who developed an equation for water profile across a side weir on the assumption that total energy along the side weir is constant. A review of previous studies indicated that rectangular sharp-crested side weirs have been investigated extensively, including work by Ackers (1957), Collings (1957), Frazer (1957), Subramanya & Awasthy (1972), Nandesamoorthy & Thomson (1972), Singh *et al.* (1994), Yu-Tech (1972), Cheong (1991). El-Khashab & Smith (1976), Uyumaz & Muslu (1985), Hager (1987, 1994), Helweg (1991), Agaccioglu & Yüksel (1998), Venutelli (2008) and Durga Rao & Pillai (2008). Borghei *et al.* (1999) studied the discharge coefficient for sharp-crested side weirs in subcritical flow and developed an equation for the discharge coefficient of sharp-crested rectangular side weirs. Also, in order to study the variation of the discharge coefficient along side weirs, Swamee *et al.* (1994) used an elementary analysis approach to estimate the discharge in smooth side weirs through an elementary strip along the side weir. Ranga Raju *et al.* (1979) investigated the discharge coefficient of a broad-crested rectangular side weir, based on the width of the main channel and Froude number. Ranga Raju *et al.* (1979) also reported that, for their experiments, the specific energy remained nearly constant with the maximum difference being less than 2%. Kumar & Pathak (1987) investigated the discharge coefficient of sharp and broad-crested triangular side weirs. Hager (1987) discussed the fact that, when one-dimensional analysis is used, the hydraulic characteristics of side weir flow cause an additional head change that may be either positive or negative, depending on the flow conditions. Ghodsian (2003) studied supercritical flow in rectangular side weirs. Aghayari *et al.* (2009) experimentally investigated the effect of height, width and side weir crest slope on the spatial discharge coefficient over broad-crested inclined side weirs under subcritical flow conditions in a rectangular channel. Probably one of the most important studies in a trapezoidal channel was conducted by Cheong (1991). Cheong investigated the discharge capacity of a lateral opening in a trapezoidal main channel. A review of the literature on the topic also indicates a lack of reliable information for predicting discharge over a side weir installed in a trapezoidal channel with significant

roughness. The use of trapezoidal channels for water measurement is increasing because they are more adaptable and more easily constructed than conventional rectangular flumes, even in natural rivers. Results of research on trapezoidal flumes at the Colorado State University hydraulics laboratory prior to 1959 have previously been published (Robinson & Chamberlain 1960). Since the use of trapezoidal channel is increasing, the hydraulic characteristics of the side weirs in irrigation channels need more consideration. A side weir in irrigation systems could conceivably offer certain advantages over most existing surface irrigation systems. These advantages include: (1) self-priming discharge; (2) simplicity of construction; (3) precise metering of discharge into channels; (4) adaptability into completely automated surface irrigation systems; and (5) low operating heads and hence shallower, less costly channels.

The flow over a side weir is a typical case of spatially varied flow with decreasing discharge. The existing studies of side weir flow deal mainly with the application of the energy principle. The constant energy assumption, which forms the basis of conventional side weir analysis, implies that at any section, the longitudinal component of velocity vector of the spill flow is equal to the average velocity of flow in the main channel. Therefore, the total energy per unit mass of water remaining in the channel is unaffected by the spill flow occurring and, apart from frictional losses, the total energy of the flow in the main channel remains constant. However, El-Khashab & Smith (1976) reported that the specific energy could decrease by as much as 5% across a side weir in a rectangular channel. The concept of constant specific energy (De Marchi 1934) is often adopted when studying the flow characteristics of these weirs (for example, Subramanya & Awasthy 1972; Ranga Raju *et al.* 1979; Hager 1987; Kumar & Pathak 1987; Cheong 1991; Singh *et al.* 1994; Borghei *et al.* 1999). In the energy principle, the slope of the water profile can be expressed as:

$$\mathrm{d}y/\mathrm{d}x = \frac{(S_0 - S_\mathrm{f}) - \alpha Q(\mathrm{d}Q/\mathrm{d}x)\left(1/gA^2\right)}{1 - \left(\alpha Q^2 T/gA^3\right)} \tag{1}$$

where T is the top width of the water surface, S_f is the average frictional slope, S_0 is the slope of the main channel, A is the area of flow in the main channel, α is the energy friction

factor, dQ/dx is the discharge per unit length over side weir, dy/dx is the slope of the water surface profile over side weir, Q is the discharge in the main channel, g is the acceleration due to gravity and y is the flow depth at a distance x from upstream of the weir (Section 1). Assuming that $S_f - S_0 = 0$ (i.e. constant specific energy across the weir) and $\alpha = 1$, the discharge q over a unit length of side weir of height P is:

$$q_s = -\frac{dQ}{dx} = \frac{2}{3}\sqrt{2g}\,C_M(y - P)^{1.5} \tag{2}$$

where x is the horizontal distance from upstream of the weir, q_s is the spill discharge per unit length of the side opening, P is the crest height of the side weir, y is the depth of flow at the section x (at $x = 0$: $y = y_1$ and $Q = Q_1$), $(y–P)$ is the pressure head on the weir, and C_M is the discharge coefficient (De Marchi coefficient) of the side weir (see Figure 1). Most previous studies focused on side weirs installed in rectangular channels. The same, however, is not true for side weirs in the trapezoidal channel. Among recent research, few previous studies have been reported on side weirs in trapezoidal channels. This paper investigates the discharge coefficient of side weirs in trapezoidal channels for a subcritical flow regime.

Using dimensional analysis, C_M can be expressed as:

$$C_M = f(Fr_1, P/y_1, B/y_1, S_0, \sigma, L/B) \tag{3}$$

The above functional relationship has been developed in the present study, in which S_0 is the main channel slope, P is the weir height, B is the main channel width, L is the length of the side weir and y_1 is the depth of the flow at the upstream section of the side weir, σ is the surface tension and Fr_1 is Froude number at the upstream end of the side
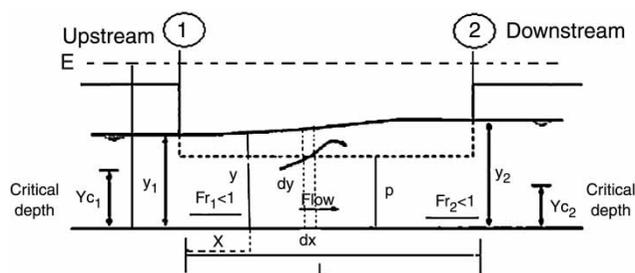
weir. Most research has used Froude number at the upstream end of the side weir at the channel center because flow at the channel center is more stable than at the bank of the weir (for example, Subramanya & Awasthy 1972; Ranga Raju *et al.* 1979; Singh *et al.* 1994; Agaccioglu & Yüksel 1998; Emiroglu *et al.* 2010). Borghei *et al.* (1999) stated that the influence of the channel slope (S_0) is very small and negligible. Coleman & Smith (1923) stated that the minimum nape height over side weirs should not be less than 19 mm because of the surface tension over the weir crest.

MATERIAL AND METHODS

Experimental setup

The experiments were carried out at the laboratory of Soil Conservation and Watershed Management Research Institute (SCWMRI) of Tehran, Iran. The experimental setup consisted of a main channel and a lateral channel (Figure 2). The main channel was 30 m long and the channel had a trapezoidal cross section. The main channel was 0.6 m deep with a 0.001 bed slope. The channel was constructed from earthen material. A combination of small coarse gravel and sand were mixed to provide the roughness coefficient of about 0.02 which is a usual manning roughness coefficient in earth channels (Chow 1959). Figure 2 shows the sieve analysis graph of the bed material. In Figure 3, d_{50} and the geometric standard deviation of the material are 0.68 cm and 2.2 respectively. In order to obtain the required roughness coefficient, d_{50} of bed material was first estimated by the Strickler formula, which is the most popular formula for estimating Manning's coefficient in natural streams (Subramanya 1986). Afterwards, the bed material was mixed together so that the required d_{50} of the bed material which was obtained by the Strickler formula was nearly reached. The roughness coefficient was also checked with the Gauckler–Manning formula. Figure 4 shows the main channel section with two different widths of 1 and 1.65 m respectively. The lateral channel was 1.5 m wide and 0.8 m deep, and was situated parallel to the main channel. A rectangular weir was placed at the end of the lateral channel in order to measure the discharge of the side weir. A point gauge with ± 0.1 mm sensitivity was placed at 0.5 m from the

Figure 1 │ Longitudinal flow profile at a side weir under subcritical condition.

Figure 2 | Laboratory setup.

Figure 3 | Sieve analysis of the bed material graph.

weir. A concrete side weir with a length of 4 m and width of 23 cm was constructed at a distance of 12.88 m from the upstream inlet. The inlet discharges were measured via a rectangular sharp crested weir. A calibrated standard rectangular was installed at the beginning of the main channel which is used to adjust inlet flow to an accuracy of ±0.1 L/s. Water was supplied to the main channel from a large 2 m deep feeding basin. Water depth measurements were conducted using point gauges installed at the side weir region and the center line of the main channel. A special

type of movable car which can move in both x and y directions on a rail were used to measure depth of flow. Eight pizometers were installed on the center line of the side weir to measure pressure values. Six series of experiments were conducted for the widths of $B = 1$, 1.25 and 1.65 m of the main channel and the side weir with the heights of $P = 0.05$ and 0.08 m. The lateral slope of the main channel was also 1(vertical):2(horizontal). A sluice gate was fitted at the end of the main channel in order to control the depth of flow as the downstream boundary condition.

Figure 4 | The main channel with two different base widths.

At the beginning of the experiments the sluice gate was closed. Then, flow with low discharges was directed into the main channel until the bed materials were well saturated. Afterwards, the discharges were increased little by little to prevent significant bed deformation. Also, at the beginning of the channel, two stone steps were made to dissipate the momentum of the inlet discharge. Since discharges were increased slowly, movement of the bed material, especially at high discharges, could almost be ignored. These actions were performed to prevent any significant bed deformation as previous research shows (for example, Rosier *et al.* 2005), significant movement of the bed material can be crucial in the functioning of the lateral weir. Nearly 90 experiments were conducted at subcritical flow and stable flow conditions. The results were analyzed and proposed as a series of equations for measuring discharge in a trapezoidal channel and mainly irrigation systems. Table 1 summarizes some of the most significant

Table 1 | Some of the most significant research for prediction of side weir coefficient under subcritical conditions

Investigators	Range of P (m)	Equation	P/y_1	Range of L(m)	Range of Froude number
Subumanya & Awasthy (1972)	$0 < P < 0.6$	$C_M = 0.611\sqrt{1 - \left(\dfrac{3Fr_1^2}{2 + Fr_1^2}\right)}$	0–0.96	0.1–0.15	0.02–0.85
Yu-Tech (1972)	–	$C_M = 0.622 - 0.222Fr_1^2$	–	–	–
Nandesamoorthy & Thomson (1972)	–	$C_M = 0.432\sqrt{\dfrac{2 + Fr_1^2}{1 + Fr_1^2}}$	–	–	–
Ranga Raju *et al.* (1979) for Sharp crested Weir	$0 < P < 0.5$	$C_M = 0.81 - 0.6Fr_1$	–	0.2–0.5	0.1–0.5
Ranga Raju *et al.* (1979) for Broad crested Weir	$0 < P < 0.5$	$C_M = (0.81 - 0.60Fr_1)\left(0.80 + 0.1\dfrac{y_1 - P}{b}\right)$	–	0.2–0.5	0.1–0.5
Hager (1987)	$P = 0$	$C_M = 0.485\sqrt{\dfrac{2 + Fr_1^2}{2 + 3Fr_1^2}}$	0	1	0–0.87
Cheong (1991)	$P = 0$	$C_M = 0.45 - 0.22Fr_1^2$	0	0.277–0.97	0.286–784
Singh *et al.* (1994)	–	$C_M = 0.33 - 0.18Fr_1 + 0.49(P/y_1)$	0.42–0.85	–	0.23–0.43
Jalili & Borghei (1996)	–	$C_M = 0.71 - 0.41Fr_1 - 0.22(P/y_1)$	–	–	–
Borghei *et al.* (1999)	$0 < P < 0.19$	$C_M = 0.7 - 0.48Fr_1 - 0.3(P/y_1) + 0.06(L/B)$	–	0.2–0.7	0.1–0.9

equations for the prediction of side weir discharge coefficient in subcritical condition. Table 2 shows the range of experimental variables.

It is clear that in most of the fundamental research concerning side weir coefficients in subcritical conditions, the upstream Froude number is introduced as the main dimensionless parameter and the proposed equations are based on the variation of the upstream Froude number. However, Singh *et al.* (1994) introduced (P/y_1) as another effective parameter on side weir coefficient. Borghei *et al.* (1999) have concluded that for a more accurate equation to predict discharge coefficient of side weir, the effects of the upstream Froude number (P/y_1) and (L/B) should be considered together.

Table 2 │ Range of test variables

Parameters	Value
Weir length L (cm)	400
Weir height P (cm)	5 and 8
Channel slope S_0 (%)	0.001
Inlet discharge (L/sec)	30–112
B (cm)	100, 125, 165
Number of runs	92

RESULTS

Water surface profiles

To describe the flow condition in the main channel, water levels were measured to obtain the water surface profiles along both the main channel centerline and the weir-side of the main channel. The depths were measured from 88 cm before the upstream edge of the side weir to 88 cm after the downstream of the side weir at 10 cm intervals by means of a point gage with ±0.1 mm sensitivity. Figure 5 shows the water surface profile along the main channel centerline and the weir-side of the main channel for $Q_S = 25$ L/sec, $Q_{in} = 110$ L/sec and $Fr_1 = 0.53$. Figure 5 shows that the flow condition at the center line of the main channel is more stable than the flow condition at the weir side of the main channel. The same situation is observed in all experimental runs. Water surface profiles alongside weirs drop slightly at the upstream end of the weir crest. This is due to the side weir entrance effect at the upstream end. Then, the water level rises quickly toward the downstream.

Longitudinal hydrostatic pressure profiles

The values of hydrostatic pressure were measured on the center line of the side weir by means of eight piezometers
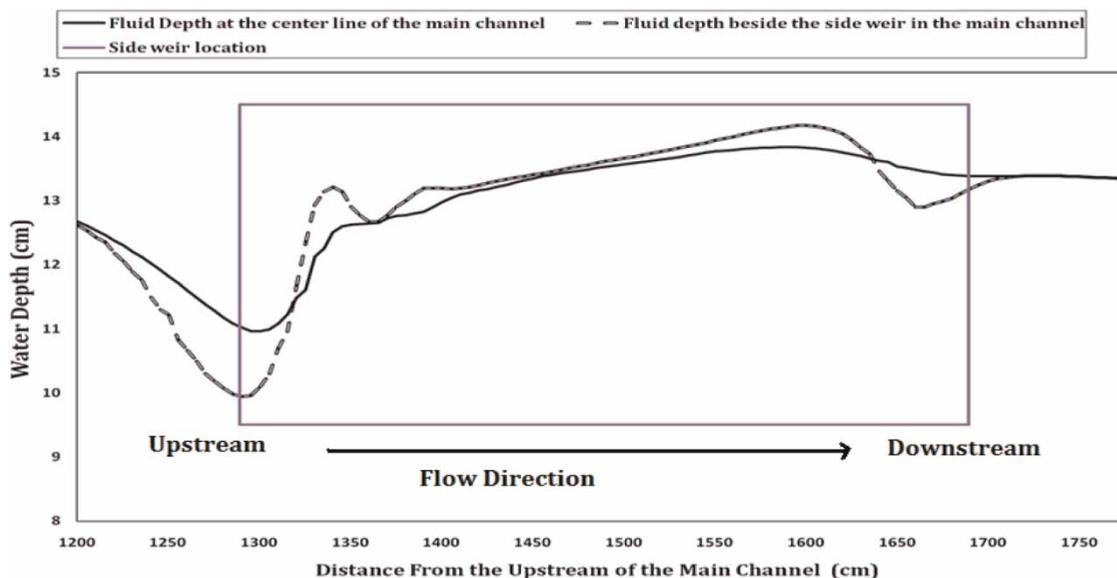

Figure 5 │ Water surface profile in the main channel and beside the side weir for $Q_S = 25$ L/sec, $Q_{in} = 110$ L/sec and $Fr_1 = 0.53$ from the beginning of the main channel.

which were installed on the center line of the side weir. These measurements were 25 cm from the upstream and downstream edge of the weir, between them 70 cm intervals start and include the weir length. Figure 6 shows a typical longitudinal hydrostatic pressure profile along the length of the weir crest for side weir with a height of 8 cm. As is clear in Figure 6, the typical pressure profiles are similar to Figure 1, which is for a subcritical condition. Figure 7 shows a typical longitudinal water surface profile along the length of the weir crest for a side weir with the height of 8 cm, $Q_S = 25$ L/sec, $Q_{in} = 110$ L/sec and $Fr_1 = 0.53$. In Figure 7, the upstream and downstream and the flow direction is also shown by following the location of the falling water into the lateral channel. It is obvious that the flow is increasing toward the downstream of the side weir. A separation zone and reverse flow were also observed at the downstream end of the side weir. Similar findings were reported by Agaccioglu & Yüksel (1998) and Emiroglu *et al.* (2010). However, it should be mentioned that the
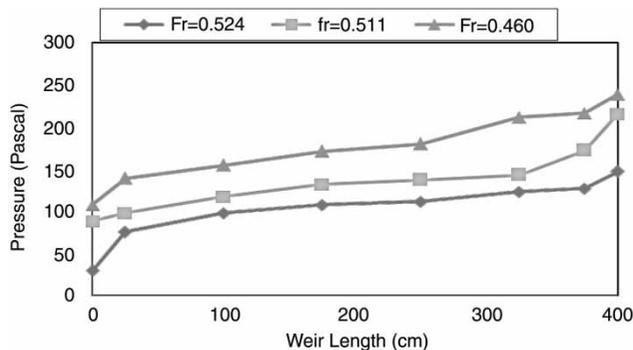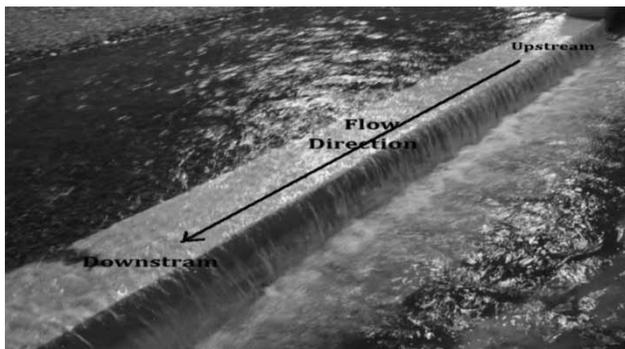
separation zone was too small in comparison with the length of the side weir. Therefore, the effect of it on the velocity distribution and the estimation of specific energy can be disregarded.

As mentioned previously, De Marchi assumed that the specific energy remains constant along the side weir. Therefore, the present data were used in order to examine this assumption. As mentioned above, most previous studies used the depth of flow at the upstream end of the side weir at the center of the channel due to the stable flow conditions (for example, Subramanya & Awasthy 1972; Hager 1987, 1994; Singh *et al.* 1994; Borghei *et al.* 1999). Therefore, the same flow depth (y_1) as in the literature has been taken into account in this study. Thus, the findings of the current study can be compared to those of previous studies within the literature. Figure 8 shows the comparison of specific energy upstream (E_1) and downstream (E_2) of the side weir with a height of 5 cm and the main channel with a width of 1 m. As is clear in Figure 8, the average energy difference between the two ends of the side weir is about 1.15% so the specific energy is almost constant. Therefore, the assumption of constant energy is accepted for further analysis. It also shows that the separation zone does not affect the specific energy.

It is shown that C_M is a function of different parameters such as Fr_1, P/y_1, B/y_1, L/B. However, with the help of the experimental results, the effect of variables was tested, either one by one or altogether, and finally the best equation is suggested. The first step would be to find out the effect of the most influential parameter. Figure 9 shows variation of discharge coefficient of the side weir for different values of upstream Froude number (Fr_1). It can be seen that as
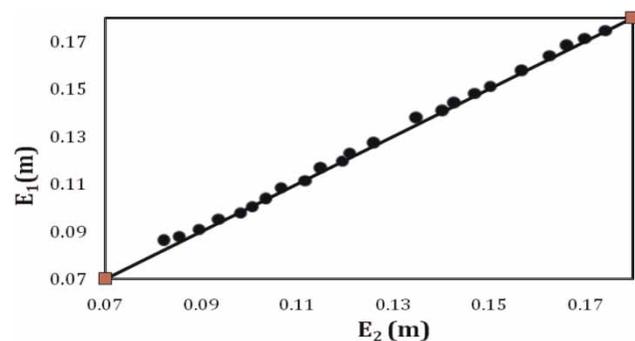

Figure 6 │ Longitudinal hydrostatic pressure distribution profile.

Figure 7 │ Water surface profile at the side weir for $Q_S = 25$ L/sec, $Q_{in} = 110$ L/sec and $Fr = 0.53$.

Figure 8 │ Comparison of specific energy E_1 and E_2 for the side weir with a height of 5 cm and the channel with a width of 1 m.
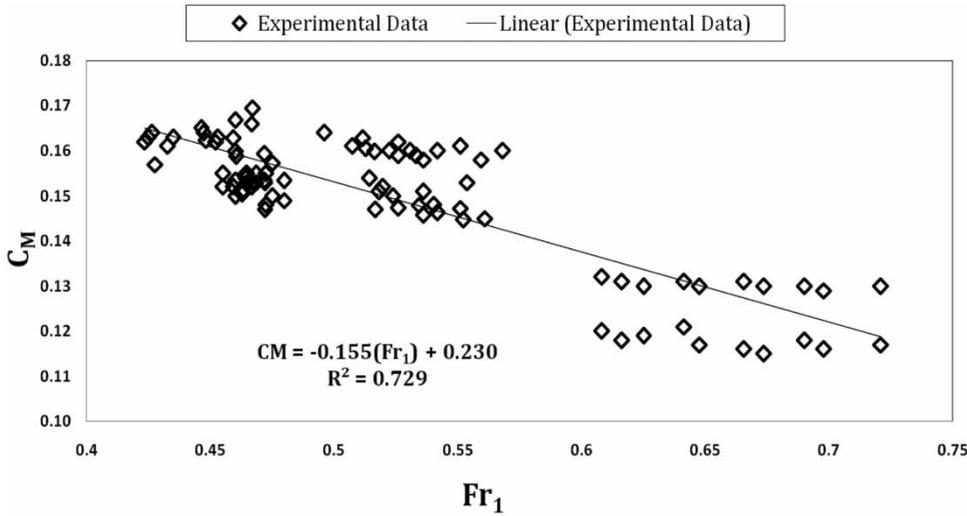
Figure 9 │ C_M for different values of Fr_1.

the upstream Froude number increases, the C_M values decrease. In other words, higher C_M values are obtained at low upstream Froude number due to increase of flow depth and decrease of flow velocity. Figure 10 shows variation of discharge coefficient of the side weir against different L/B ratios. It can be seen that, as the L/B ratio increases, the C_M values also increase. Increase of C_M values must be due to the existence of secondary flow created by lateral flow. El-Khashab & Smith (1976) pointed out that the secondary flow condition due to lateral flow is dominant when a side weir is relatively long (i.e. $L/B > 1$).

To study the effect of P/y_1 ratio on the C_M, the values of C_M are plotted against P/y_1 in Figure 11. As can be seen in Figure 11, C_M values decreases with an increase in P/y_1.

Figure 12 shows the variation of discharge coefficient of the side weir against the ratio of the main channel width to

the upstream flow depth (B/y_1). As shown in Figure 12, when the ratio of B/y_1 increases, the C_M values also increase. It is because of the increase in the channel width. As the channel width increases, the water depth decreases which will decrease the lateral discharge.
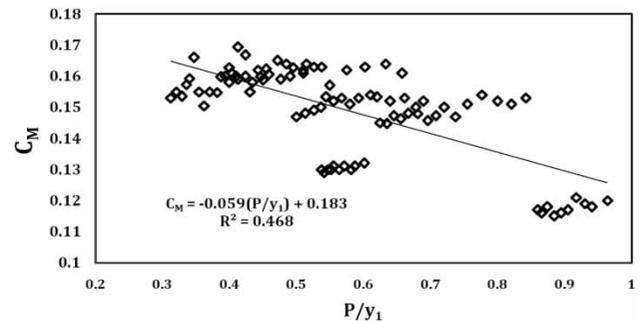
Figure 11 │ C_M for different values of P/y_1.
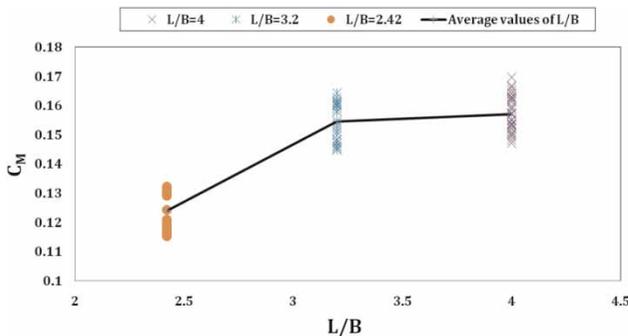

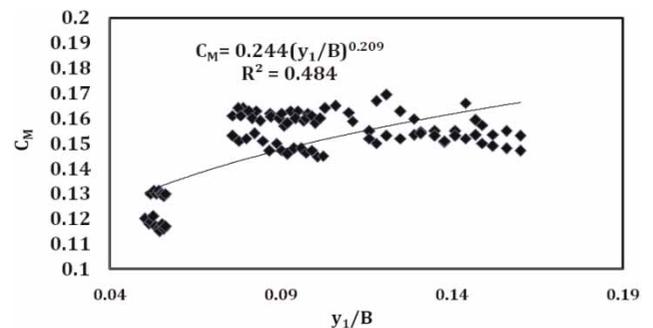**Figure 10** │ C_M for different values of L/B.

Figure 12 │ C_M for different values of y_1/B.

It is clear that the upstream Froude number is the most significant parameter, as other researchers declared. After studying the effect of the dimensionless parameters on C_M, the combination of these parameters will also be studied. Figures 13–16 show C_M values as a function of (y_1/B, P/y_1), (Fr_1, y_1/B), (Fr_1, p/y_1) and (Fr_1, y_1/B, P/y_1), respectively. Figure 17 also shows the computed values of C_M against the measured values C_M for all of the parameters. Table 3 shows the percentage difference in using each equation compared to the actual measured discharge. It is clear that the influence of L/B is very important.

As is clear in Table 3, the regression equation of the best-fit line which is obtained from the combination of all four parameters is found to be:

$$C_M = -0.036(P/y_1)^{1.286} + 0.186(Fr_1)^{-0.117}$$
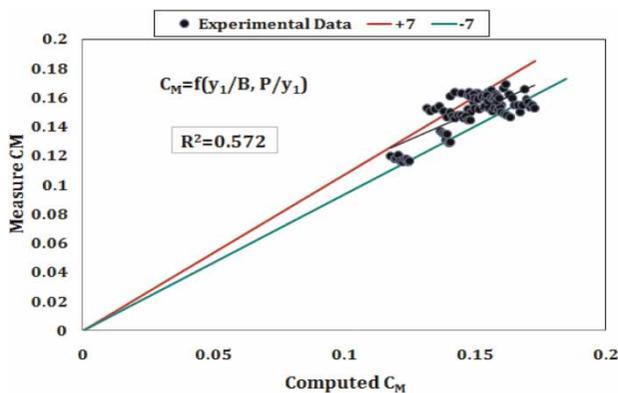$$- 0.214(y_1/B)^{0.952} - 4.137(L/B)^{-5.472} \qquad (4)$$
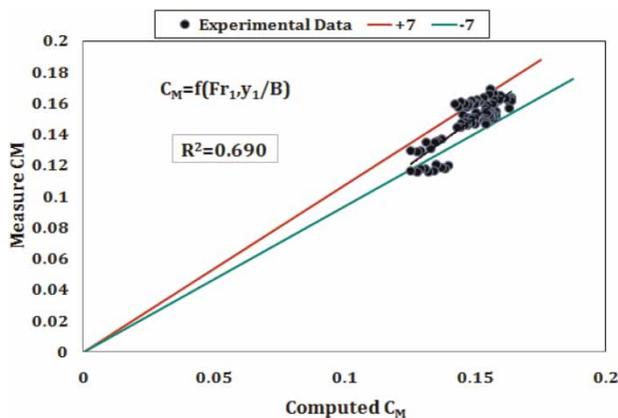

Figure 13 | C_M as a function of (y_1/B, P/y_1).
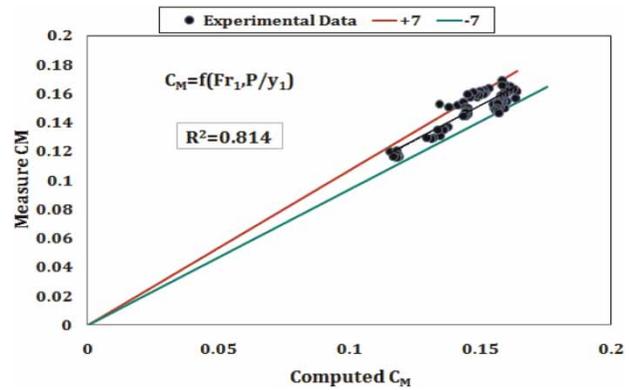

Figure 14 | C_M as a function of (Fr_1, y_1/B).

Figure 15 | C_M as a function of (Fr_1, P/y_1).
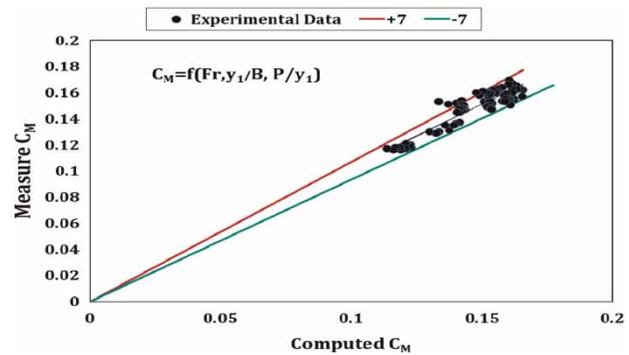

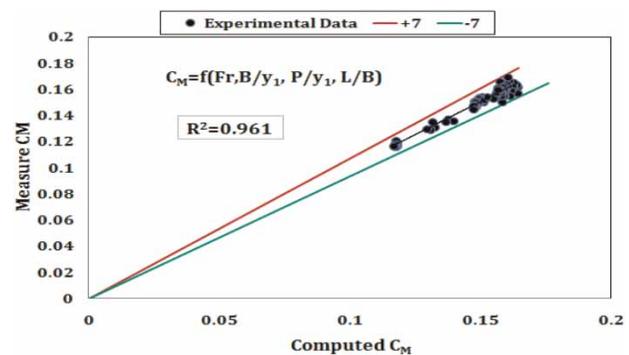**Figure 16** | C_M as a function of (Fr_1, y_1/B, P/y_1).

Figure 17 | Computed values of C_M against the measured values of C_M.

In Figure 18, experimental data and some of the other researchers' formulas in which C_M is a function of Fr_1 are compared. As is clear in Figure 18, the predicted values of C_M by other researchers' equations are higher than the experimental values. This is because of the different experimental conditions. As mentioned before, although Cheong

Table 3 | Percentage difference between calculated and measured discharge using different equations

$C_M = f()$	Difference (%)	R^2	Equation
Fr_1	4.2	0.722	$C_M = -0.154(Fr_1) + 0.230$ (5)
P/y_1	6.1	0.479	$C_M = -0.059(P/y_1) + 0.183$ (6)
Y_1/B	6.3	0.484	$C_M = 0.244(y_1/B)^{0.209}$ (7)
P/y_1, Fr_1	3.1	0.814	$C_M = -0.031(P/y_1)^{5.203} + 0.114(Fr_1)^{-0.442}$ (8)
P/y_1, y_1/B	5.1	0.572	$C_M = -0.05(P/y_1)^{0.965} + 0.233(y_1/B)^{0.115}$ (9)
Fr_1, y_1/B	4.3	0.690	$C_M = -0.235(Fr_1)^{0.411} + 0.320(y_1/B)^{-0.011}$ (10)
Y_1/B, Fr_1, P/y_1	2.9	0.849	$C_M = -0.036(P/y_1)^{2.071} - 0.234(Fr_1)^{0.442} + 0.309(y_1/B)^{-0.035}$ (11)
Y_1/B, Fr_1, P/y_1, L/B	1.3	0.961	$C_M = -0.036(P/y_1)^{1.286} + 0.186(Fr_1)^{-0.117} - 0.214(y_1/B)^{0.952} 4.137(L/B)^{-5.472}$ (12)
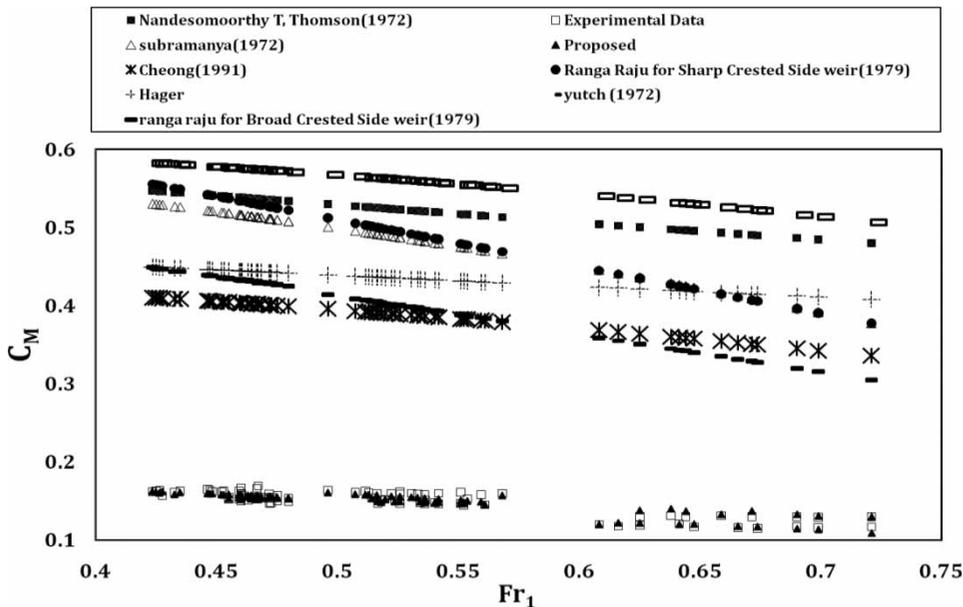
Figure 18 | Experimental values of C_M against researchers' formulas in which C_M is a function of Fr_1.

performed his experiments in a trapezoidal channel, they have been done for a lateral opening, the weir has a height of zero. Because of the absence of weir height in Cheong experiments, the amount of discharge which was diverted into the lateral channel was more in comparison of the condition in which the weir has height. A weir with any height other than zero will perform as a barrier and will allow less flow to go through the side weir, particularly for low discharges. So by using the Cheong equation, the predicted values of C_M show further values than the experimental data. The other reason is roughness of the main channel and the side weir itself, which is made up of concrete.

Also, the side weir is broad-crested which will pass less flow into the lateral channel in comparison to a sharp-crested side weir based on the studies of Ranga Raju *et al.* (1979). Therefore, Ranga Raju's equation for a broad-crested weir is closer to experimental data than Ranga Raju's other equation for a sharp-crested weir. As mentioned before, the different conditions of other experiments to the current experiments, such as the ratio of L/B, cross section of the main channel, roughness of the bed material, roughness of the side weir crest and type of the side weir crest (side-weir crest shape), have caused a significant difference between predicted and measured values of C_M. Also, it
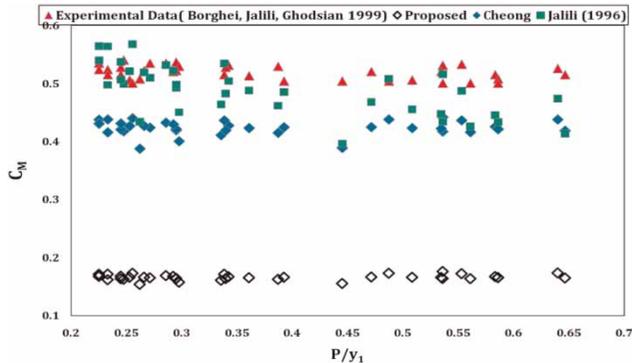
Figure 19 | Comparison of Borghei's experimental data with Cheong (1991), Jalili & Borghei (1996) and Equation (8).

should be mentioned that although maximum attempts have been made to prevent the movement of bed material, it is impossible to prevent the movement of bed material completely, especially at high discharges. Therefore, the lateral outflow may also be affected. However, the other researchers' formulas were obtained at fixed bed conditions.

Comparison of the proposed equation with other formulas

The experimental data of Borghei *et al.* (1999) was used in order to compare the proposed equation with other researchers' formulas. In this comparison Cheong's formula (1991) and Jalili & Borghei's equations (1996) were also used. Figure 18 shows the result of the comparison of Borghei's experimental data with Cheong (1991), Jalili & Borghei (1996) and the proposed equations. As can be seen in Figure 19, the proposed equation predicts C_M values lower than the Cheong and Jalili's equations. Cheong's equation also predicts C_M values lower than the experimental and Jalili's equation.

CONCLUSION

Laboratory experiments were carried out using a side weir located in an earthen trapezoidal channel in order to investigate the effect of the dimensionless parameters Fr_1, P/y_1, B/y_1, L/B on discharge coefficient. The following conclusions can be drawn from these findings:

- It has been shown that De Marchi's equation for flow over a side weir in an earthen trapezoidal channel can be used

to estimate the discharge coefficients of a side weir discharging from a main channel into a lateral channel.

- The discharge coefficients of the side weir have much lower values than those of the other researchers' formulas. This is because of different experimental conditions between other researchers' experiments and the current experiments, such as the ratio of L/B, cross section of the main channel, roughness of the bed material, roughness of the side weir crest and type of the side weir crest.

- It was seen that the upstream Froude number is the most significant parameter. The values of the discharge coefficient C_M decrease with an increase in Fr_1 and p/y_1. Moreover, the discharge coefficient C_M increases with increasing L/B and y_1/B ratios.

- The longitudinal pressure profile at the center line of the side weir was analyzed. It was seen that the pressure distribution is the function of the downstream and the upstream Froude number and, for the subcritical condition, it will increase from upstream of the side weir towards the downstream of the side weir.

REFERENCES

Ackers, P. 1957 A theoretical consideration of side weirs as storm water overflow. *Proc. ICE, London* **6**, 250–269.

Agaccioglu, H. & Yüksel, Y. 1998 Side weir flow in curved channels. *J. Irrig. Drain. Eng. ASCE* **124** (3), 163–175.

Aghayari, F., Honar, T. & Keshavarzi, A. 2009 A study of spatial variation of discharge efficient in broad-crested inclined side weirs. *Irrig. Drain.* **58**, 246–254.

Borghei, M., Jalili, M. R. & Ghodsian, M. 1999 Discharge coefficient for sharp crested side weir in subcritical flow. *J. Hydraul. Eng. ASCE* **125** (10), 1051–1056.

Cheong, H. 1991 Discharge coefficient of lateral diversion from trapezoidal channel. *J. Irrig. Drain. Eng.* **117** (4), 461–475.

Chow, V. T. 1959 *Open Channel Hydraulics*. McGraw-Hill, New York.

Coleman, G. S. & Smith, D. 1923 The discharging capacity of side weirs. *Proc. ICE, London* **6**, 288–304.

Collings, V. K. 1957 Discharge capacity of side weir. *Proc. Inst. Civ. Eng.* **6**, 288–304.

De Marchi, G. 1934 Saggio di teoria de funzionamente degli stramazzi letarali. *L'Energia Elettrica* **11** (11), 849–860.

Durga Rao, K. H. V & Pillai, C. R. S. 2008 Study of flow over side weirs under supercritical conditions. *Water Resour. Manage.* **22**, 131–143.

El-Khashab, A. & Smith, K. V. H. 1976 Experimental investigation of flow over side weirs. *J. Hydraul. Eng. ASCE* **102** (9), 1255–1268.

Emiroglu, M. E., Kaya, N. & Agaccioglu, H. 2010 Discharge capacity of labyrinth side weir located on a straight channel. *J. Irrig. Drain. Eng. ASCE* **136** (1), 37–46.

Frazer, W. 1957 The behavior of side weirs in prismatic rectangular channels. *Proc. Inst. Civ. Eng.* **6**, 305–327.

Ghodsian, M. 2003 Supercritical flow over rectangular side weir. *Can. J. Civ. Eng.* **30** (3), 596–600.

Hager, W. H. 1987 Lateral outflow over side weirs. *J. Hydraul. Eng. ASCE* **113** (4), 491–504.

Hager, W. H. 1994 Supercritical flow in circular-shaped side weirs. *J. Irrig. Drain. Eng.* **120** (1), 1–17.

Helweg, O. J. 1991 *Microcomputer Applications in Water Resources*. Prentice-Hall, Englewood Cliffs, NJ.

Jalili, M. R. & Borghei, S. M. 1996 Discussion of discharge coefficient of rectangular side weir by R. Singh, D. Manivannan and T. Satyanarayana. *J. Irrig. Drain. Eng. ASCE* **122** (2), 132.

Kumar, C. P. & Pathak, S. K. 1987 Triangular side weirs. *J. Irrig. Drain. Eng.* **113** (1), 98–105.

Nandesamoorthy, T. & Thomson, A. 1972 Discussion of spatially varied flow over side weir. *J. Hydraul. Eng. ASCE* **98** (12), 2234–2235.

Ranga Raju, K. G., Prasard, B. & Gupta, S. K. 1979 Side weir in rectangular channel. *J. Hydraul. Div. ASCE* **105** (5), 547–554.

Robinson, A. H. & Chamberlain, A. R. 1960 Trapezoidal measuring flumes for open-channel flow measurement. *Trans. ASAE* **3** (2), 120–124.

Rosier, B., Boillat, J. L. & Schleiss, A. J. 2005 Influence of side overflow induced local sedimentary deposit on bed form related roughness and intensity of diverted discharge. *Proc. XXXI IAHR Congress*, September 11–16, 2005, Seoul, Korea.

Singh, R., Manivannan, D. & Satyanarayana, T. 1994 Discharge coefficient of rectangular sides. *J. Irrig. Drain. Eng. ASCE* **120** (4), 814–819.

Subramanya, K. 1986 *Flow in Open Channels*. Tata McGraw-Hill Education, New Delhi.

Subramanya, K. & Awasthy, S. C. 1972 Spatially varied flow over. *J. Hydraul. Div. ASCE* **98** (1), 1–10.

Swamee, P. K., Santosh, K. P. & Masoud, S. A. 1994 Side weir analysis using elementary discharge coefficient. *J. Irrig. Drain. Eng. ASCE* **120** (4), 742–755.

Uyumaz, A. & Muslu, Y. 1985 Flow over side weir in circular channels. *J. Hydraul. Eng.* **111** (1), 144–160.

Venutelli, M. 2008 Method of solution of nonuniform flow with the presence of rectangular side weir. *J. Irrig. Drain. Eng. ASCE* **134** (6), 840–846.

Yu-Tech 1972 Discussion of spatially varied flow over side weir. *J. Hydraul. Eng.* **98** (11), 2046–2048.